



Invited review

Cannabinoid 2 receptor is a novel anti-inflammatory target in experimental proliferative vitreoretinopathy[☆]

Anna-Maria Szczesniak^{a,*,1}, Richard F. Porter^{a,1}, James T. Toguri^a,
Joanna Borowska-Fielding^a, Simon Gebremeskel^c, Anuja Siwakoti^{b,c}, Brent Johnston^c,
Christian Lehmann^{a,b,c,d}, Melanie E.M. Kelly^{a,b,e}

^a Departments of Pharmacology, Dalhousie University, Halifax, NS, Canada

^b Departments of Anesthesia, Dalhousie University, Halifax, NS, Canada

^c Departments of Microbiology and Immunology, Dalhousie University, Halifax, NS, Canada

^d Departments of Physiology and Biophysics, Dalhousie University, Halifax, NS, Canada

^e Departments of Ophthalmology and Vision Sciences, Dalhousie University, Halifax, NS, Canada

ARTICLE INFO

Article history:

Received 7 February 2016

Received in revised form

18 August 2016

Accepted 24 August 2016

Available online 25 August 2016

Keywords:

Proliferative vitreoretinopathy

Endocannabinoid system

Cannabinoid 2 receptor

Inflammation

Anti-inflammatory agents

ABSTRACT

Proliferative vitreoretinopathy (PVR) can develop after ocular trauma or inflammation and is a common complication of surgery to correct retinal detachment. Currently, there are no pharmacological treatments for PVR. Cannabinoids acting at cannabinoid 2 receptor (CB2R) can decrease inflammation and fibrosis. The objective of this study was to examine the anti-inflammatory actions of CB2R as a candidate novel therapeutic target in experimental PVR. PVR was induced by intravitreal injection of dispase in wild-type (WT) and CB2R genetic knockout (CB2R^{-/-}) mice. Ocular pathology was studied at 24 h or one week after dispase injection. CB2R modulation was examined in WT mice, using the CB2R agonist, HU308, and the CB2R antagonist, AM630. Histopathological scoring and quantification of microglia was used to evaluate tissue pathology. Quantitative PCR and multiplex assays were used to assess changes in proinflammatory cytokines. Intravital microscopy (IVM) was used to visualize and quantify leukocyte-endothelial adhesion to the iridial microcirculation. Activation of CB2R with HU308 in WT mice with PVR decreased mean histopathological scores, the number of microglia, and leukocyte adhesion compared to vehicle-treated animals. Conversely, an increase in histopathological scores and activated microglia was observed in PVR animals after treatment with AM630. CB2R^{-/-} mice with PVR exhibited exacerbated ocular histopathology, increased microglia numbers, and elevated protein levels of cytokines as compared to WT mice. In conclusion, our results indicate that intervention at early stage PVR with CB2R agonists reduces ocular inflammation and disease severity. CB2R may represent a therapeutic target to prevent PVR progression and vision loss.

This article is part of the Special Issue entitled 'Lipid Sensing G Protein-Coupled Receptors in the CNS'.

Crown Copyright © 2016 Published by Elsevier Ltd. All rights reserved.

Contents

1. Introduction	628
2. Materials and methods	629
2.1. Animals	629
2.2. Induction of PVR	629
2.3. PVR assessment	629
2.4. Induction of endotoxin-induced uveitis	629

[☆] Supported by an operating grant to MEMK from the Canadian Institutes of Health Research (MOP-97768). Richard Porter was funded by a scholarship from the Dalhousie University Department of Ophthalmology and Visual Science: Dr. R. Evatt and Rita Mathers Graduate Scholarship.

* Corresponding author. Department of Pharmacology, Dalhousie University, 5850 College Street, Halifax, NS, B3H 4R2, Canada.

E-mail address: anna.maria.szczesniak@dal.ca (A.-M. Szczesniak).

¹ These authors contributed equally to the work presented here and should be regarded as equivalent authors.

2.5.	Immunohistochemistry	629
2.6.	Quantitative reverse transcription polymerase chain reaction	629
2.7.	Measurement of inflammatory markers	629
2.8.	Intravital microscopy	630
2.9.	Cannabinoid treatments	630
2.10.	Statistical analysis	630
3.	Results	630
3.1.	Dose-dependent disease induction of PVR	630
3.2.	CB2R activation reduces PVR histopathology and Iba-1 positive MG accumulation	630
3.3.	CB2R activation reduces leukocyte-endothelial interactions in the iridial microcirculation	633
3.4.	Genetic loss of CB2R exacerbates PVR pathology	633
4.	Discussion	633
4.1.	The role of CB2R in the inflammatory response	634
4.2.	Effects of CB2R modulation on MG function	636
4.3.	Effect of CB2R modulation on leukocyte-endothelial interactions	636
	Conflict of interest	636
	Supplementary data	636
	References	636

1. Introduction

Proliferative vitreoretinopathy (PVR) is an inflammatory and fibrotic ocular disease. It can develop after ocular trauma, and is a common complication of surgery to correct a retinal detachment in around 5 to 10 percent of patients (Pastor, 1998). PVR is characterized by the growth and proliferation of contractile epiretinal membranes that cause traction within the vitreous, leading to recurrent retinal detachments (Mandava et al., 2002). Epiretinal membranes are comprised of extracellular matrix proteins and migrated cells including retinal pigment epithelial cells, glial cells, fibroblasts, and macrophages (Lei et al., 2007). Immune cells that have been identified in the pathogenesis of PVR include neutrophils, microglia (MG) and macrophages (Tan et al., 2012). Vitreous surgery is the standard treatment of care, with the goal of closing all retinal breaks and removing epiretinal membranes (Pastor, 1998; Sadaka and Giuliari, 2012). The success rate for PVR treatment is moderate and in some patients the disease eventually culminates in vision loss (Patel et al., 2004). Currently, there are limited pharmacological therapies for the treatment of PVR (Khan et al., 2015). Corticosteroids are commonly used and while these drugs do suppress the immune response, they have many adverse systemic and ocular effects including, increased intraocular pressure, risk of glaucoma, and cataracts. Further effort is needed to develop alternative non-steroidal treatment options (Kersey and Broadway, 2006).

The endocannabinoid system (ECS) is an emerging target in the treatment of inflammatory and fibrotic diseases (Akhmetshina et al., 2009; Munoz-Luque et al., 2007; Rajesh et al., 2010). The ECS is an endogenous lipid signaling system comprised of two identified G protein-coupled receptors, cannabinoid receptor type 1 (CB1R) and cannabinoid receptor type 2 (CB2R), endogenous lipid ligands, including *N*-arachidonylethanolamine (AEA) and 2-arachidonoyl glycerol (2-AG), and enzymes responsible for endocannabinoid synthesis and degradation (Kreitzer and Stella, 2009; McPartland et al., 2015; Mechoulam and Parker, 2013). 2-AG is a full agonist at CB2R (Gonsiorek et al., 2000), with activation inhibiting adenylyl cyclase and stimulating mitogen-activated protein kinases. CB1R is expressed on both pre- and post-synaptic nerve terminals throughout the central nervous system (CNS) and in the periphery. CB2R is often referred to as the “peripheral cannabinoid receptor”, since it is highly expressed on immune cells (Galiege et al., 1995; Munro et al., 1993), and drugs acting at this

receptor lack behavioral side-effects associated with cannabinoids that act at CB1R (Morales et al., 2016). CB2R has also been reported in peripheral and CNS tissues (Lu et al., 2000), including retina (Lu et al., 2000), and endothelium (Schley et al., 2009). The presence of CB2R on both innate and adaptive immune cells, such as neutrophils, mast cells, natural killer cells, monocytes, microglia, B cells, and T cells suggests that this receptor may be a potential target for immunomodulation (Rom et al., 2013; Tanasescu and Constantinescu, 2010). In support of this, receptor mRNA expression is highly induced during inflammatory conditions (Maresz et al., 2005; Storr et al., 2009), and activation of CB2R has been reported to be anti-inflammatory in experimental models of sepsis (Lehmann et al., 2012, 2011), uveitis (Toguri et al., 2014), rheumatoid arthritis, multiple sclerosis (MS), Alzheimer's disease (AD), Huntington's disease (HD), Parkinson's disease (PD), head injury, and ischemia-reperfusion (Downer, 2011).

The involvement of the ECS, and more specifically, CB2R, in retinitis has not been extensively investigated. However, Xu et al. (2007), using a model of autoimmune uveoretinitis, reported that modulation of the ECS, and in particular activation of CB2R, was anti-inflammatory; a mechanism that involved inhibition of the activation and function of autoreactive T cells and a reduction in leukocyte recruitment to the inflamed retina (Xu et al., 2007). More recent work by our group (Toguri et al., 2014), using a rodent model of endotoxin-induced uveitis (EIU), has indicated that activation of CB2R reduces leukocyte-endothelial interactions, and decreases the levels of pro-inflammatory cytokines (interleukin 1- β [IL-1 β], interleukin-6 [IL-6], tumor necrosis factor [TNF], interferon- γ [INF- γ], chemokine [C-C motif] ligand 5 [CCL5], chemokine [C-X-C motif] ligand 2 [CXCL2]) and transcription factors responsible for production of pro-inflammatory mediators (nuclear factor-kappaB [NF- κ B], activator protein 1 [AP-1]). This latter study also demonstrated that in EIU, CB2R agonists were more efficacious than clinically used topical agents, including steroids and NSAIDs. Taken together, these studies contribute to the growing field of research into the immunomodulatory properties of cannabinoids and their potential to treat inflammatory disease, including in the eye.

The purpose of this study was to examine the role of CB2R in experimental PVR. We used the CB2R selective cannabinoid agonist, HU308, and antagonist, AM630, as well as CB2R genetic knockout (CB2R^{-/-}) mice, together with histopathology, immunohistochemistry, cytokine analysis and intravital microscopy (IVM), to evaluate the role of CB2R in PVR pathology.

2. Materials and methods

2.1. Animals

Male C57BL/6 wild-type (WT; 20–25 g; Charles River, QC, Canada) age 6–8 weeks and CB2R^{-/-} mice on C57BL/6J background were used for experiments. CB2R^{-/-} mice were purchased from Jackson Laboratories (Bar Harbour, USA), and were bred *in house*. Age-matched male CD1 mice (20–25 g; Charles Rivers, QC, Canada) were used for intravital microscopy (IVM) experiments as the absence of pigment allowed for visualization of leukocyte-endothelial interactions in the iridial microvasculature. BALB/c mice (20–25 g; Charles River) were used for the EIU study to determine the optimal dose for HU308. Animals were maintained on a 12 h light/dark cycle, with unrestricted access to food and water. All experiments were conducted in accordance with the standards and procedures of the Canadian Council on Animal Care and were approved by the Dalhousie University Committee on Laboratory Animals. All studies involving animals are reported in accordance with the ARRIVE guidelines for reporting experiments involving animals (<http://www.nc3rs.org.uk/>; [Kilkenny et al., 2010](#); [McGrath et al., 2010](#)).

2.2. Induction of PVR

PVR was induced in mice, as previously described ([Cantó Soler et al., 2002](#)), using an intravitreal injection of dispase (Sigma, St. Louis, MO, USA), a neutral protease which cleaves basement membrane. Dispase was diluted to a concentration of either 0.1U/μl or 0.2U/μl in a sterile saline solution. Under general anesthesia, animals were injected intravitreally with sterile saline or dispase solution (2 μl) using a 30G needle and Hamilton syringe (Hamilton Company, Reno, NV, USA) with assistance of a WILD M37 dissecting microscope (Leitz Canada, Kitchener, ON, Canada). Anesthesia was induced by 4.0% isoflurane, maintained using 2% isoflurane (both in 70% N₂O/30% O₂), and monitored by toe pinch. Once the injection was completed, the puncture wound was glued shut with 3M Vetbond Tissue Adhesive (3M Animal Products, St. Paul, MN, USA), and animals were allowed to recover.

At one week post-injection, C57BL/6 and CB2R^{-/-} mice were sacrificed by an intraperitoneal (i.p.) overdose of sodium pentobarbital (250 mg/kg), eyes were enucleated and prepared for histological or immunohistochemical staining, as well as mRNA extraction for quantitative polymerase chain reaction (qPCR). For IVM, CD1 mice were injected with 0.2U/μl of dispase or sterile saline and the iridial microcirculation was imaged 24 h post-injection. For IVM, BALB/c mice were injected with 125 μl of LPS and the iridial microcirculation was imaged 6 h post-injection.

2.3. PVR assessment

The internal tissue morphology of the eye was visualized by haematoxylin and eosin (H&E) staining under a light microscope (Wild Leitz, Willowdale, ON, Canada). The severity of the disease was scored on a scale from 0 (no disease) to 4 (maximum disease) in one-point increments, according to a semi-quantitative pathophysiological scale (Table 1) modified from [Agarwal et al. \(2012\)](#), one week following intravitreal injection.

2.4. Induction of endotoxin-induced uveitis

EIU was induced in BALB/c mice, as previously described ([Toguri et al., 2014](#)), using an intravitreal injection of LPS (2 μl; 125 ng/μl; *E. coli* 026:B6 L8274; Sigma). The iridial microcirculation was imaged using IVM at 6 h post-injection.

Table 1

Evaluation of experimental PVR was based on histological examination of retinal sections according to a modified histological scoring table from [Agarwal et al. \(2012\)](#).

Histopathology	Description
0	No disease, normal retinal architecture
1	Retinal layers clearly visible Inflammatory cell infiltration (inner retina layer)
2	Focal retinal detachments Retinal layers still visible Moderate inflammatory cell infiltration Localized retinal folds
3	Retinal layers poorly distinguishable Immune cell infiltration throughout retinal layers Extensive retinal folds Granulomas
4	Full thickness retinal damage Severe inflammatory cells infiltration Large granulomatous lesions

2.5. Immunohistochemistry

Eyes were enucleated and immersed in 4% paraformaldehyde in 0.1 M phosphate buffer for 24 h. Fixed eyes were then transferred into 30% sucrose in phosphate buffer saline (PBS) for cryoprotection. Symmetrical sagittal sections (14 μm) of the whole eye were cut on a freezing microtome (Leica CM1850 cryostat; Leica Microsystems Inc., Concord, ON, Canada), and collected on the microscope slides (Superfrost/Plus, Fisher). For immunohistochemical staining, slides were washed in PBS (3 × 15min), then incubated for 1 h at room temperature with 10% normal goat serum (Vector Labs) and 0.3% Triton™ X-100 (Sigma Aldrich) in PBS. This step was followed by overnight incubation of sections, at 4 °C, with the anti-rabbit Iba-1 (marker of MG and macrophages) or anti-GFAP (marker for astrocytes) (Wako Chemicals, USA; 1: 100) primary antibody. Fluorescent-tagged antibody CY™³ goat anti-rabbit IgG (1:500, Jackson ImmunoResearch Laboratories, West Grove, PA), was used for visualization of Iba-1 and GFAP. Immunohistochemical controls were performed by omission of either the primary or the secondary antibodies. Iba-1-positive cells were enumerated using a Nikon C1 fluorescence microscope under 40X magnification. For each retina, 5–10 sections on one slide (and representing a cross-section of the whole retina) were counted and averaged. Iba-1 staining in retina is selective for microglia and macrophages, and has been used by us and others in previous publications ([Maneu et al., 2014, 2016](#)).

2.6. Quantitative reverse transcription polymerase chain reaction

Total RNA was harvested from freshly isolated retina samples using Qiagen plus RNA isolation kit (Qiagen, Mississauga, ON). Reverse transcription was carried out using 1 μg RNA and cDNA was prepared using iScript cDNA synthesis kit (Biorad, Mississauga, ON). Quantitative PCR was performed in duplicate with 1 μl of cDNA using Quantifast SYBR Green (Qiagen). Amplification was performed using a RG-6000 Rotor-Gene (Corbett, Mississauga, ON) and analyzed using the 2^{-ΔΔCT} relative quantification technique ([Gebremeskel et al., 2015](#)) and expressed relative to internal normalizing standard mRNA level. High-stringency primers ([Supplementary Table 1](#)) were used for examining the expression of Iba-1 (MG, macrophages), GFAP (astrocytes), CD68 (monocytes/macrophages), Ly6G (neutrophils), IL-1β, IL-6. Quantitative reverse transcription polymerase chain reaction (qPCR) data were normalized to the expression of glyceraldehyde-3-phosphate dehydrogenase (GAPDH).

2.7. Measurement of inflammatory markers

Measurement of inflammatory markers was conducted as

previously described, (Toguri et al., 2014). Frozen whole globes were homogenized in 100 μ L of PBS and 1% bovine serum albumin, supplemented with a protease inhibitor cocktail (Sigma, St. Louis, MO, USA). Homogenates were centrifuged at 13,000 $\times g$ for 15 min at 4 °C, and supernatant was collected. The Bio-Rad Protein Assay (Mississauga, ON) was used to determine protein concentration according to the manufacturer's instructions. Protein was diluted to a concentration of 3620 μ g/ml in PBS then diluted 1:1 in mice diluent provided within the Procarta Multiplex Cytokine Assay Kit (Freemont, CA, USA). Samples were analyzed using a Bio-Rad 200 instrument with Bio-Plex software (Mississauga, ON). Samples were run in duplicate to examine levels of IL-1 β and IL-6. Standard curves were generated for each cytokine using the reference standards supplied with the kit.

2.8. Intravital microscopy

IVM was conducted as previously described (Toguri et al., 2014). Briefly PVR was induced in CD1 mice 24 h prior to IVM, following the same protocol as described above (0.2 U dispase). Animals were anesthetized with pentobarbital (i.p. 54 mg/kg). 15 min before initiating IVM, Rhodamine 6G (i.v. 1.5 ml/kg; Sigma-Aldrich, ON, Canada) was injected to visualize leukocytes within the vasculature, while fluorescein isothiocyanate (FITC) conjugated albumin (i.v. 1 ml/kg; Sigma-Aldrich, ON, Canada) allowed visualization of blood flow. The iridial microcirculation was observed using an Olympus OV100 Small Animal Imaging System (Olympus, Tokyo, Japan). Images were captured in real-time by a black and white DP70 CCD C-mount camera and digitally recorded with Wasabi software (Hamamatsu, Herrsching, Germany). During IVM the eye was observed in four quadrants. Two to four videos of each quadrant were recorded for 30 s each. Videos were analyzed off-line without knowledge of the treatment groups. Adherent leukocytes were defined as the number of leukocytes during the 30 s observation period that did not detach from the endothelial surface. Using imaging software (ImageJ; National Institute of Health, USA) the number of adherent leukocytes within each vessel segment was calculated by measuring the diameter and length of vessel segment studied, assuming a cylindrical geometry of blood vessels. Adherent leukocytes were expressed as number of cells per mm² of endothelial surface.

2.9. Cannabinoid treatments

The CB2R agonist, HU308 (4-[4-(1,1-dimethylheptyl)-2,6-dimethoxyphenyl]-6,6-dimethylbicyclo[3.1.1]hept-2-ene-2-methanol), and the CB2R antagonist, AM630 (6-Iodo-2-methyl-1-[2-(4-morpholinyl)ethyl]-1H-indol-3-yl](4-methoxyphenyl)methanone), were purchased from Tocris Bioscience (Bristol, UK), and were dissolved in dimethyl sulfoxide (DMSO) (Sigma Aldrich, ON, Canada) and sterile saline (3:7) for i.p. administration. In C57BL/6 mice with PVR, HU308 was administered daily for 7 days at the dose of 1 mg/kg (100 μ L/animal). The CB2R antagonist, AM630, was administered for 7 days i.p. to C57BL/6 mice with PVR at the dose of 2.5 mg/kg (100 μ L). Control animals received daily i.p. injections (100 μ L) of the vehicle (DMSO/saline; 3:7).

For IVM, animals were injected with two i.v. doses (at 0 and 12 h) of either, HU308 (1 mg/kg; 100 μ L), AM630 (2.5 mg/kg; 100 μ L) or vehicle (DMSO/saline; 3:7), following intravitreal dispase injection (0.2U/ μ L). In BALB/c mice with EIU, HU308 was administered i.v. at a dose of 0.1–10 mg/kg (100 μ L/animal) directly after intravitreal injection of LPS (250 ng). Control animals received i.v. 100 μ L DMSO and saline (3:7).

2.10. Statistical analysis

Individual animals in each treatment group were coded and experiments were analyzed by two independent blinded observers. All data are expressed as mean \pm standard deviation (SD), and results were analyzed using Prism 5 software (GraphPad Software, La Jolla, CA, USA). Following confirmation of normal distribution of data by Kolmogorov-Smirnov testing, Student's *t*-test was used to compare two groups and one-way analysis of variance (ANOVA) with a Tukey's *post hoc* test was used for multiple comparisons. Significance was set at $p < 0.05$.

3. Results

3.1. Dose-dependent dispase induction of PVR

The first objective was to establish and score our model of PVR using different concentrations of intravitreal dispase compared to saline control injections (Fig. 1). Histological scoring of retinal tissue morphology was assessed from eyes enucleated one week following the intravitreal injection of 2 μ L of dispase at different concentrations (0.1U, 0.15U, 0.2U, 0.4U per μ L) or saline (control). Fig. 1A and B shows representative H&E staining of cross sections of the globe (top panel) and retinal section (bottom panel) from control animals one week after receiving an intravitreal injection of saline. Control eyes appeared histopathologically normal with no overt pathology and with clearly distinct retinal layers (histopathological score 0; Table 1). Fig. 1C and D shows H&E staining of a representative cross section of the globe and a retinal section, respectively, one week post-intravitreal injection of 0.15U dispase. The representative retinal section shown (Fig. 1D) received a histopathological score of 2 (Table 1). Retinal layers are clearly visible, but there is inflammatory cell infiltration and localized retinal folds are present (left direction arrow). Fig. 1E and F shows representative H&E staining of a cross section of the globe and a retinal section one week after intravitreal injection of 0.2U dispase. A histopathological score of 4 (Table 1) was assigned due to the presence of poorly distinguishable retinal layers, extensive retinal folds, retinal detachments (right direction arrow) and large granulomas lesions (Fig. 1F). H&E staining in eyes enucleated one week after injection with 0.4U dispase showed such extensive PVR damage that they could not be accurately scored, as per Table 1. These retinal sections also showed signs of retinal hemorrhage (data not shown).

The histogram in Fig. 1G shows PVR scores at one week post-intravitreal injection with 0.1U, 0.15U or 0.2U dispase compared to control (intravitreal saline injection). The histopathological score was significantly increased ($p < 0.001$) following injection with either 0.15U (2.88 ± 1.12) or 0.2U dispase (3.75 ± 0.5) in comparison to the control saline-injected group (0.25 ± 0.5).

For experiments examining whether pharmacological block or loss of CB2R increased the severity of PVR histopathology, a dose of 0.1U dispase was used as this dose produced only minimal pathology. For examining the putative anti-inflammatory actions of CB2R activation, a dose of 0.2U dispase was used. This dose of dispase generated more severe PVR scores.

3.2. CB2R activation reduces PVR histopathology and Iba-1 positive MG accumulation

To assess the involvement of CB2R in mitigating PVR damage, mice were treated with a selective CB2R agonist, HU308. The histogram in Fig. 2A shows that activation of the CB2R with daily i.p. 1.0 mg/kg HU308 significantly reduces the mean histopathological score compared to treatment with vehicle, $p < 0.01$. This dose has been shown to be efficacious in reducing leukocyte adhesion to the

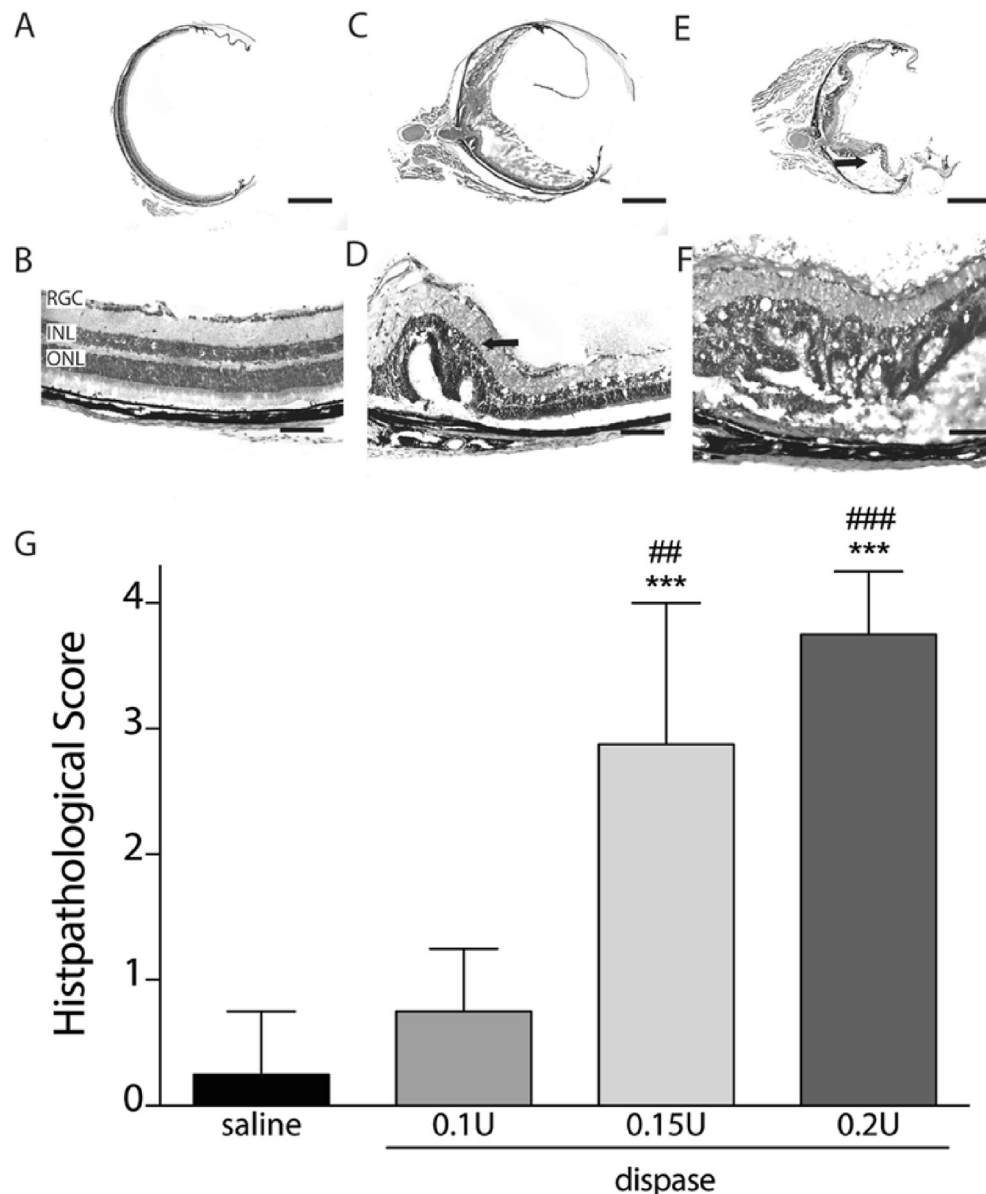


Fig. 1. Dispase induces dose-dependent experimental PVR in mice. H&E staining of representative globe cross-sections (top panel, 2.5x magnification) and retinal sections (bottom panel, 20x) from WT mice at one week post-intravitreal injection of (A & B) saline, (C & D) dispase (0.15U), or (E & F) dispase (0.2U). Labelled retina: retinal ganglion cell layer (RGC), inner neuronal layer (INL), outer neuronal layer (ONL), retinal folds (□), retinal detachment (►). Scale bar = 400 μ m (top panel), 100 μ m (bottom panel). (G) Bar graph represents mean histopathological scores (according to Table 1) for the following groups: Saline ($n = 4$), 0.1U dispase ($n = 4$), 0.15U ($n = 8$), 0.2U dispase ($n = 4$). *** $P < 0.001$ compared with saline, ## $P < 0.01$ and ### $P < 0.001$ compared to 0.1U dispase.

iridial microcirculation during EIU (Supplementary Fig. 1). Mice treated with 0.2U dispase plus HU308 had a histopathological score of 2.0 ± 1.0 , while mice treated with 0.2U dispase plus vehicle had a histopathological score of 3.75 ± 0.5 ($p < 0.01$). Mice treated with saline plus vehicle also had a significant decrease in the mean histopathological score compared to 0.2U dispase plus vehicle, ($p < 0.01$). There was no significant difference in the mean histopathological scores between mice treated with saline plus vehicle or HU308 (data not shown). The beneficial effect of HU308 was blocked by pre-treatment of the animals with selective CB2R antagonist, AM630, with a resultant histopathological score of 3.88 ± 0.4 ($p < 0.01$). Furthermore, eyes from animals injected with 0.1U dispase and treated with the CB2R antagonist, AM630 (Fig. 2B; i.p. 2.5 mg/kg), exhibited a significantly worse mean histopathological score compared to vehicle-treated animals ($p < 0.01$). Mice

treated with the CB2R antagonist, AM630, had a histological score of 3.12 ± 0.5 whilst vehicle-treated mice had a histopathological score of 0.75 ± 0.5 . In the presence of the CB2R antagonist, AM630, HU308 treatment did not improve the mean histopathological score induced by 0.1 U dispase (3.4 ± 0.5 ; $p < 0.01$).

Fig. 3 shows representative staining of Iba-1 positive cells (MG and macrophages) in retinal sections from eyes with PVR, induced by the intravitreal injection of 0.2U dispase, plus daily i.p. treatment with vehicle (Fig. 3A) or 1.0 mg/kg HU308 (Fig. 3B). In vehicle-treated mice (Fig. 3A), retinal MG have an amoeboid-like appearance, consistent with activation (Walter et al., 2003), and are found throughout the retina. When mice are treated with HU308 (Fig. 3B), MG exhibit a ramified morphology and are confined largely to the inner retina, suggesting a resting or inactive MG phenotype (Stence et al., 2001). Fig. 3C and D shows representative staining of Iba-1

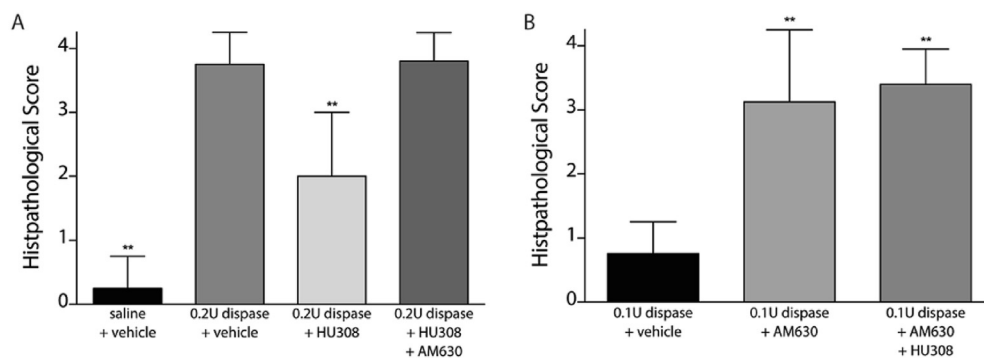


Fig. 2. CB2R pharmacological modulation modifies PVR pathology. Bar graphs represent the mean histopathological scores (according to Table 1) from WT mice at one week post-intravitreal injection of saline or dispase (0.1U or 0.2U) and daily treatment for 7 days with either: (A) vehicle ($n = 4$), the CB2R agonist HU308 (1.0 mg/kg; $n = 5$) or HU308 plus the CB2R antagonist AM630 (2.5 mg/kg; $n = 5$), (B) vehicle ($n = 4$), AM630 (2.5 mg/kg; $n = 8$) or AM630 plus HU308 (1.0 mg/kg; $n = 5$). ** $P < 0.001$ compared with dispase + vehicle.

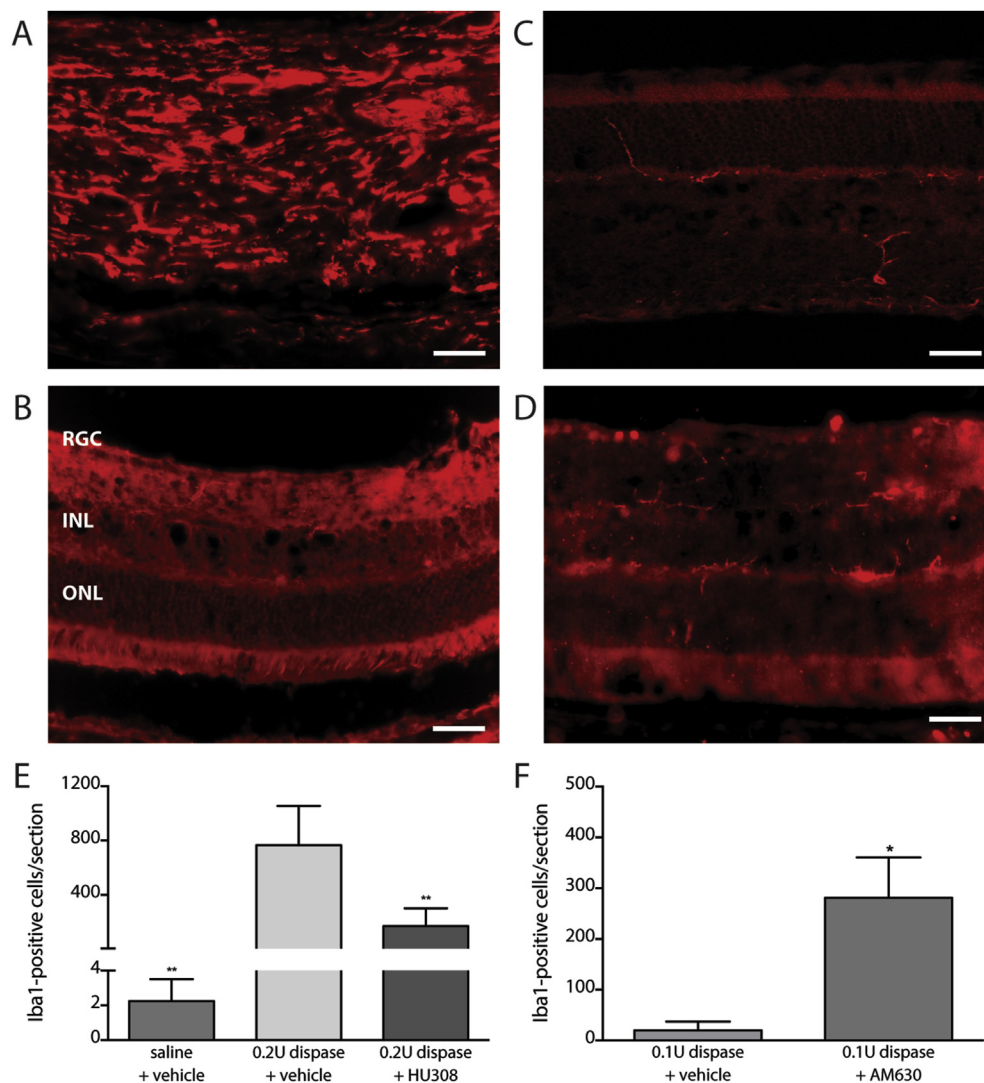


Fig. 3. CB2R activation reduces number of retinal MG/macrophages in PVR. Representative anti-Iba-1 staining of retinal sections from WT mice one week after intravitreal injection of: (A) 0.2U dispase + vehicle (i.p. once daily), (B) 0.2U dispase + HU308 (i.p. once daily; 1.0 mg/kg), (C) 0.1U dispase + vehicle (i.p. once daily), (D) 0.1U dispase + AM630 (i.p. once daily; 2.5 mg/kg). Labelled retina: retinal ganglion cell layer (RGC), inner neuronal layer (INL), outer neuronal layer (ONL). Scale bar = 40 μ m. (E) Bar graph represents the mean number of MG per 5–10 retinal sections/animal for the following groups: saline + vehicle ($n = 4$), saline + HU308, 0.2U dispase + vehicle ($n = 4$), 0.2U dispase + HU308 ($n = 5$). (F) Bar graph represents the mean number of Iba-1-positive cells per 5–10 retinal sections/animal for the following groups: 0.1U dispase + vehicle ($n = 4$), 0.1U dispase + AM630 ($n = 5$). * $P < 0.05$, ** $P < 0.01$ compared with dispase + vehicle.

positive cells in retinal sections from eyes with PVR, induced by intravitreal injection of 0.1U dispase, plus daily i.p. treatment with vehicle (Fig. 3C) or 2.5 mg/kg AM630 (Fig. 3D). The histogram in Fig. 3E shows that mice treated with an intravitreal injection of 0.2U dispase plus HU308 (daily i.p. 1.0 mg/kg) had significantly fewer Iba-1 positive cells (171 ± 131 MG per section) than retinal sections from animals treated with 0.2U dispase plus vehicle (766 ± 289 MG per section; $p < 0.01$). Fig. 3E shows that mice treated with an intravitreal injection of saline plus vehicle (daily i.p.) had significantly fewer Iba-1-positive cells (2 ± 1 MG per section) than retinal sections from animals treated with 0.2U dispase plus vehicle ($p < 0.01$). There was no difference in Iba-1 positive cells per retinal section compared to saline plus HU308 (data not shown). Fig. 3F shows that the mean number of Iba-1-positive MG in retinal sections one week after the intravitreal injection of 0.1U dispase in WT animals treated daily with i.p. AM630 was significantly increased (281 ± 17 MG per section) compared to eyes from vehicle-treated animals (20 ± 17 MG per section; $p < 0.05$).

3.3. CB2R activation reduces leukocyte-endothelial interactions in the iridial microcirculation

IVM was performed to examine leukocyte-endothelial adhesion in the iridial microcirculation 24 h following intravitreal injection of saline, 0.2U dispase plus vehicle or dispase plus CB2R agonist (HU308) (Fig. 4). Eyes with intravitreal injection of 0.2U dispase plus i.v. treatment with vehicle (100 μ l) had significantly more leukocytes (577 ± 313 cells/mm²) adhering to the iridial endothelium compared to control eyes that received only intravitreal saline injection (127 ± 15 cells/mm²; $p < 0.01$). Consistent with the anti-inflammatory effect of CB2R activation, i.v. treatment with the CB2R agonist, HU308 (1.0 mg/kg), significantly attenuated dispase-induced leukocyte-endothelial interactions at 24 h (230 ± 146 cells/mm²), as compared to vehicle-treated animals ($p < 0.01$). Mice treated with the CB2R antagonist, AM630 (2.5 mg/kg), following intravitreal injection of 0.2U dispase, showed exacerbated leukocyte-endothelial interactions, but could not be accurately quantified due to the excessive number of adherent fluorescently-labelled cells (data not shown).

3.4. Genetic loss of CB2R exacerbates PVR pathology

To further examine the involvement of CB2R in PVR

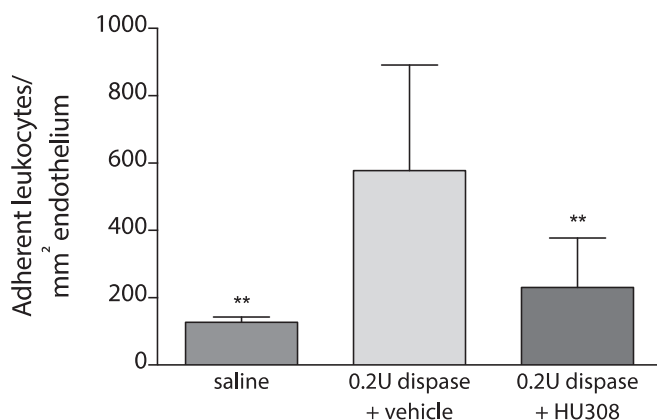


Fig. 4. CB2R activation reduces leukocyte-endothelial interactions in the iridial microcirculation in PVR. Bar graph represents the mean number of adherent leukocytes 24 h after intravitreal injection of: Saline ($n = 7$), 0.2U dispase + i.v. vehicle ($n = 8$), or 0.2U dispase + i.v. HU308 (1.0 mg/kg; $n = 9$). ** $P < 0.01$ compared to 0.2U dispase + vehicle.

pathogenesis, CB2R^{-/-} mice were used for the experiments (Fig. 5). Fig. 5A shows a representative H&E staining of a cross section taken from a retina of a CB2R^{-/-} animal one week after receiving an intravitreal injection of saline. The control eyes appeared histopathologically normal (histopathological score 0; Table 1). Fig. 5B shows H&E staining of a representative cross section of a retina one week post-intravitreal injection of 0.1U dispase. The representative retinal section shown (Fig. 5B) received a histopathological score of 2 (Table 1). Retinal layers are clearly visible and the presence of localized retinal folds is evident. Fig. 5C and D shows representative staining of Iba-1-positive cells in retinal sections from CB2R^{-/-} eyes, with an intravitreal injection of saline (Fig. 5C), or 0.1U dispase (Fig. 5D). The histogram in Fig. 5E shows that CB2R^{-/-} animals injected with intravitreal 0.1U dispase have a significantly higher mean histopathological score (2.2 ± 0.45) compared to intravitreal saline-injected CB2R^{-/-} animals (0.33 ± 0.58 ; $p < 0.01$). Examination of Iba-1-positive cells in retinal sections from CB2R^{-/-} mice (Fig. 5F) one week after intravitreal injection of either saline (control) or 0.1U dispase showed that retinal sections from CB2R^{-/-} mice have significantly increased retinal Iba-1-positive cells (144 ± 87 MG per section) compared to saline controls (2 ± 1 MG per section; $p < 0.01$). Retinal Iba-1-positive cells were also significantly increased in dispase-injected CB2R^{-/-} mice compared to WT mice injected with the same dose of dispase ($p < 0.01$).

Quantitative PCR was used to examine the relative expression of mRNA for MG/macrophages (Iba-1), monocytes and macrophages (CD68), astrocytes (GFAP), neutrophils (Ly6G), and pro-inflammatory mediators IL-1 β and IL-6 in the isolated retinas of WT or CB2R^{-/-} animals one week after the intravitreal injection of saline, 0.1U or 0.2U dispase. The most applicable inflammatory molecules were chosen for measurements based on animal and clinical studies of PVR and dispase-induced inflammation (El-Ghrably et al., 2001; Kon et al., 1999; Morescalchi et al., 2013). Fig. 6 shows increased levels of relative expression of Ly6G, and IL-1 β transcripts examined in CB2R^{-/-} retinas after intravitreal injection of 0.1U dispase compared to WT with 0.1U dispase ($p < 0.05$). Supplementary Fig. 2 shows greater immunoreactivity of GFAP stained retinal sections after the intravitreal injection of 0.1U dispase compared to saline-injected animals. Pro-inflammatory cytokine measurements were also obtained from ocular tissue (intact globes) 12 h after intravitreal injection with low dose of dispase (0.1U) in WT or CB2R^{-/-} mice. The intravitreal injection of 0.1U dispase showed a greater fold change in the levels of inflammatory mediators IL-1 β and IL-6 (Supplementary Fig. 3) as compared to saline controls ($p < 0.05$). The levels of the cytokines were also significantly elevated in CB2R^{-/-} mice, as compared to WT animals ($p < 0.05$).

4. Discussion

PVR develops in response to a reparative process induced by retinal breaks and exacerbated inflammatory responses (Pastor et al., 2002). While the majority of research on PVR focuses on long term pathological changes in the retinal architecture (Cantó Soler et al., 2002; Tan et al., 2012; Zhang et al., 2012), the current study investigated the initial inflammatory response in PVR, a key stage of PVR development (Morescalchi et al., 2013). Corticosteroid anti-inflammatory drugs have been used experimentally and clinically to prevent PVR (Bali et al., 2010; Morescalchi et al., 2013), but many of these agents have well-documented adverse side-effects (Chen et al., 2011; Sadaka and Giuliani, 2012).

We focused our study on the role of CB2R in PVR, since a growing body of evidence indicates that the activation of this receptor is beneficial in a number of neuroinflammatory and neurodegenerative conditions (Ashton and Glass, 2007; Rom and

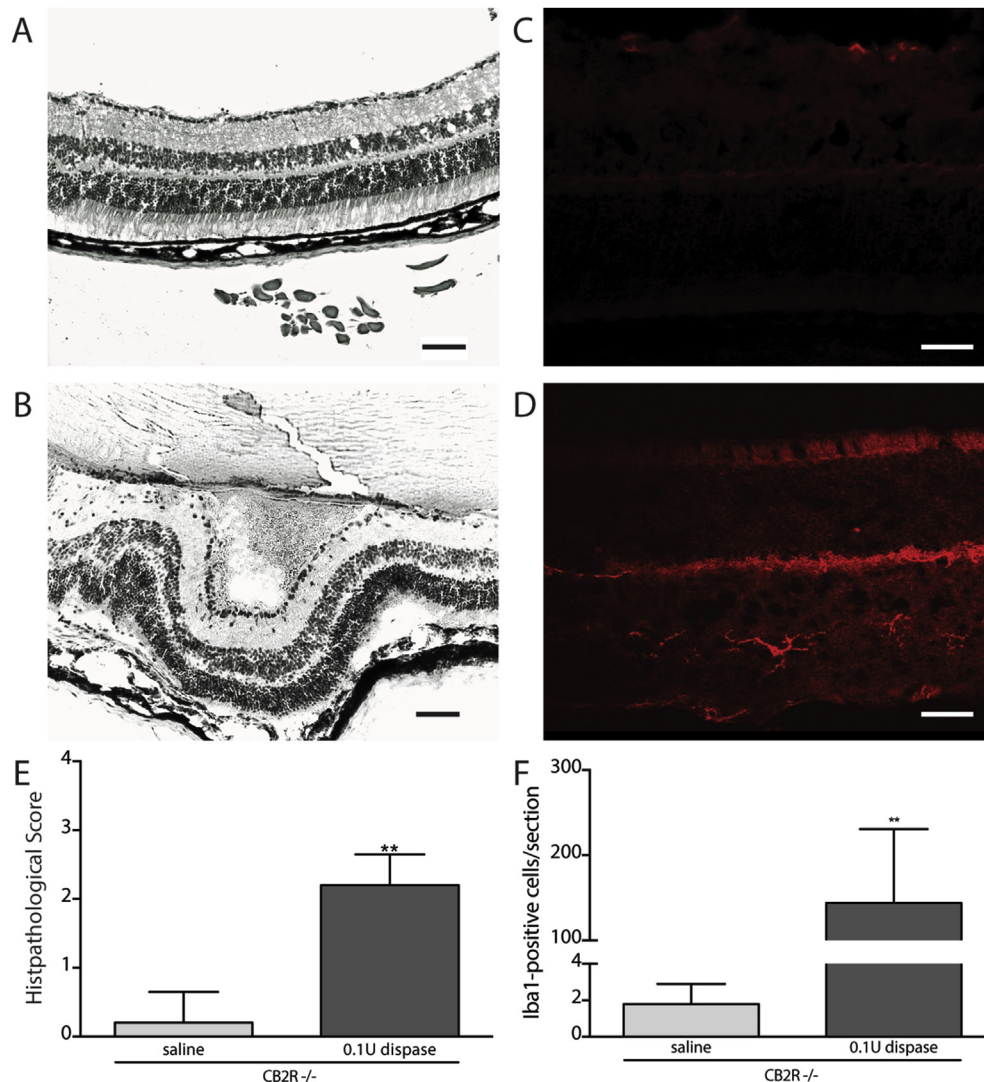


Fig. 5. $CB2R^{-/-}$ mice exhibit more severe retinal pathology and increased numbers of microglia/macrophages in PVR. Histology of the retina in mice treated with (A) saline and (B) 0.1U dispase in $CB2R^{-/-}$ mice. Iba-1 positive cells in animals treated with (C) saline and (D) 0.1U dispase. Scale bar = 100 μ m (left panel), 40 μ m (right panel). (E) Bar graph shows mean histopathological scores (according to Table 1) in $CB2R^{-/-}$ mice following intravitreal injection of either saline ($n = 5$) or 0.1U dispase ($n = 5$). (F) Bar graph represents the mean number of Iba-1-positive cells per 5–10 retinal sections/animal in $CB2R^{-/-}$ mice following intravitreal injection with either saline ($n = 5$) or 0.1U dispase ($n = 7$). $^{**}P < 0.01$ compared with saline.

Persidsky, 2013). From a therapeutic perspective, targeting $CB2R$ has a number of advantages: (1) ligands activating this receptor lack the behavioral side-effects associated with cannabinoid ligands that act at $CB1R$, (2) $CB2R$ is expressed on immune cells involved in both the innate and adaptive immune responses, including neutrophils, macrophages and microglia, natural killer cells, mast cells, B cells, and T cells, and (3) receptor expression is highly induced during inflammation (Maresz et al., 2005; Storr et al., 2009). Taken together, this suggests that drugs activating $CB2R$ may potentially limit inflammation, PVR progression and severity, while exhibiting fewer side-effects than current immunosuppressive agents.

Our study demonstrated that induction of PVR-like pathology is generated via injection of dispase into the posterior chamber of the eye. Disease severity with dispase was dose-dependent. We observed progressive pathological changes in the retinal morphology with increasing doses of dispase (0.1–0.4U), including the formation of retinal folds occurring mainly within the outer retinal layers, extensive retinal detachments, degradation of retinal

layers and infiltration of immune cells. These observations are consistent with a previously published study which used a similar PVR model (intravitreal injection of dispase at 0.2U/ μ l) and showed gradual development of PVR-like pathologies, including retinal folds, glial activation (astrocyte, MG, Müller) and MG proliferation appearing after one week, and epi- and sub-retinal membrane formation after two weeks (Pastor et al., 2002).

In our study, PVR was also associated with activation of retinal MG, with alterations in MG morphology from a resting to activated phenotype. More specifically, with dispase insult, the quiescent MG expressing a ramified phenotype changed morphology to amoeboid/phagocytic phenotype, an active state that is also associated with the synthesis and secretion of pro-inflammatory molecules (Boche et al., 2013; Morrison and Filosa, 2013; Takaki et al., 2012).

4.1. The role of $CB2R$ in the inflammatory response

In our study, we observed that activation of $CB2R$ by the selective agonist, HU308, attenuated pathological changes in retinal

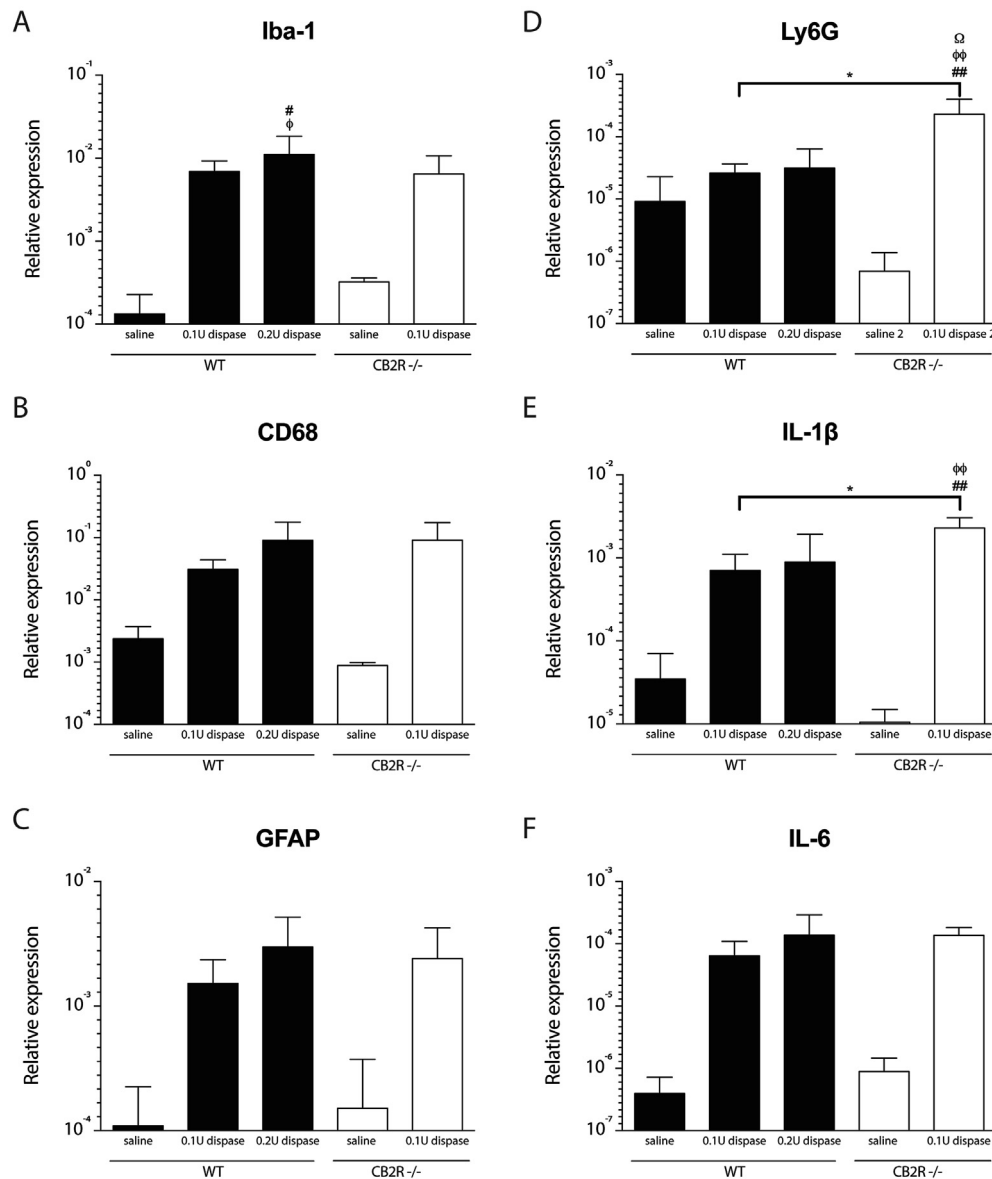


Fig. 6. WT and CB2R^{-/-} mice have an increased expression of mRNA for cells of innate immunity, including MG and macrophages (Iba1, CD68; A & B), reactive astrocytes (GFAP; C), and neutrophils (Ly6G; D), as well as pro-inflammatory mediators (IL-1β, IL-6; E & F) in PVR. Bar graphs represent relative expression of mRNA (A) Iba-1, (B) CD68, (C) GFAP, (D) Ly6G, (E) IL-1β, and (F) IL-6 transcripts by qPCR in extracts of isolated retinas from WT and CB2R^{-/-} mice one week after intravitreal injection of saline (control), 0.1U or 0.2U disperse ($n = 4$ per group). $\Phi P < 0.05$, $\Phi\Phi P < 0.01$ compared with WT + saline. * $P < 0.05$ compared with WT + 0.1U disperse. $\Omega P < 0.05$ compared with WT + 0.2U disperse. # $P < 0.05$, ## $P < 0.01$ compared with CB2R^{-/-} + saline.

tissue in PVR, and improved general retinal morphology compared to the vehicle group. This effect was negated by the pre-administration of the selective CB2R antagonist AM630, which enhanced the PVR-induced inflammatory damage. Our immunohistochemical data for Iba-1, a MG and macrophage marker, demonstrates that CB2R activation decreases the number of retinal Iba-1 positive cells as compared to the vehicle-treated group while treatment of animals with a selective CB2R antagonist, AM630, resulted in an increase in the number of these cells in ocular tissues and more pronounced tissue damage. A similar effect was also observed in the CB2R^{-/-} animals, in which the loss of endogenous CB2R activity rendered mice more susceptible to the inflammatory effects of intravitreal disperse than WT animals. Our qPCR data demonstrated alterations in the expression of mRNA levels for Iba-1 (MG and macrophages) and CD68 (MG and macrophages/monocytes) upon PVR induction. Yet, while we observed significant

increase in Iba-1 protein in CB2R^{-/-} mice, the change in mRNA expression for Iba-1, as compared to WT animals, was not evident. This finding may simply reflect the time point at which retinas were harvested, as at one week following disperse injection the inflammatory response is fully established. Interestingly our qPCR results also revealed that retinas from animals with PVR expressed significantly elevated mRNA levels for another player of innate immunity, neutrophils (Ly6G), which most likely contribute to the tissue damage we observed.

The results presented here are also consistent with previously published literature, which show that the activation of CB2R has anti-inflammatory properties in a number of *in vitro* and *in vivo* models (Rom et al., 2013; Tanasescu and Constantinescu, 2010). The activation of both CB1R and CB2R has been demonstrated to be neuroprotective in the experimental models of acute brain injury such as cerebral ischemia and traumatic brain injury (Lopez-

Rodriguez et al., 2015; Mechoulam et al., 2002), as well as in neurodegenerative disorders, including AD, MS, ALS and HD (Lopez-Rodriguez et al., 2015; Pryce and Baker, 2015; Stella, 2011; Zhang et al., 2003). Additionally, studies using mice deficient of CB2R (CB2R^{-/-}) indicated increased sensitivity to inflammatory insults in the experimental models of MS and HD (Palazuelos et al., 2009, 2008; Sagredo et al., 2009).

4.2. Effects of CB2R modulation on MG function

CB2R is expressed by MG, however, the receptor expression profile depends on the activation state of these cells (Carlisle et al., 2002). Under normal physiological conditions, CB2R mRNA is barely detectable in the CNS (Carlisle et al., 2002; Griffin et al., 1999; Schatz et al., 1997). Conversely, in inflammatory and neurodegenerative conditions, CB2R expression is considerably increased (Benito et al., 2003; Maresz et al., 2005; Carrier et al., 2004; Eljaschewitsch et al., 2006; Ramirez et al., 2005). For example, in an experimental model of encephalomyelitis, CB2R mRNA expression was 10-fold greater in activated MG cells, as compared to resting cells (Maresz et al., 2005). A number of studies have suggested that the activation of CB2R on MG increases their proliferation and motility, while reducing pro-inflammatory cytokine production. However, in our model we observed significantly fewer MG cells upon treatment with CB2R agonist HU308, and a change in MG morphology toward a basal resting state. A similar effect was reported by Lopez-Rodriguez et al. (2015), who used a murine model of traumatic brain injury to show that CB1 and CB2 receptors modulated MG activation and reactivity, with no effect on cellular proliferation (Lopez-Rodriguez et al., 2015).

Activated MG synthesize a number of pro-inflammatory mediators, including nitric oxide, IL-1 β , IL-6, TNF, and become phagocytic (Stella, 2011; Streit et al., 1999). These effects have been shown to induce neuronal damage in a number of neuroinflammatory and neurodegenerative conditions (Fernández-Ruiz et al., 2007, 2015; Kreitzer and Stella, 2009), including the disperse-induced model of PVR (Turgut et al., 2011). Both IL-1 β and IL-6 have been shown to be elevated in the vitreous of PVR patients (El-Ghrably et al., 2001), with IL-6 implicated as a predictive risk factor for the development of PVR (Kon et al., 1999). In our study, we observed IL-1 β and IL-6 protein levels to be significantly higher in WT and CB2R^{-/-} mice with PVR, as compared to both strains of mice injected with saline. Furthermore, protein levels for both cytokines were significantly increased in CB2R^{-/-} mice with PVR, as compared to WT animals. Yet, the increase in mRNA level was only statistically significant for IL-1 β . This increase in the pro-inflammatory cytokines IL-6 and IL1 β in the eyes of CB2R^{-/-} mice may contribute to the enhanced inflammatory response seen in CB2R^{-/-} in our PVR model.

Our results in experimental PVR are in line with a previous study by Toguri et al. (2014), in which increased levels of TNF, IL-6 and IL-1 β upon intraocular injection of lipopolysaccharide in rats, was attenuated by the topical application of HU308, an effect which was blocked by AM630. The decrease in pro-inflammatory cytokines by cannabinoids acting at CB2R may occur by the inhibition of transcription factors that induce cytokine gene expression. For example, TNF, a major cytokine released by MG cells in a number of pathological conditions, is inhibited by the activation of CB2R via the inhibition of NF- κ B (Rajesh et al., 2007). The synthesis of nitric oxide, another important inflammatory mediator, was also inhibited by treatment with cannabinoid agonists acting at CB1R and CB2R in MG, macrophages, astrocytes, and neurons (Martínez-Orgado et al., 2007; Shmist et al., 2006). Taken together, the anti-inflammatory effects of CB2R activation observed in this study of PVR may be attributed, in part, to decreased synthesis of some of the pro-inflammatory cytokines by reactive MG.

4.3. Effect of CB2R modulation on leukocyte-endothelial interactions

Since human PVR also affects tissues in the anterior chamber of the eye, including the iris (Aaberg, 1988; Diddie et al., 1996; Machemer et al., 1991), we took advantage of IVIM, which allowed us to non-invasively observe and quantify the behavior of leukocytes in the iridial microvasculature in live animals with PVR. Our results from these experiments indicate that the CB2R activation in PVR is important in the modulation of leukocyte adherence during the inflammatory response. We showed that intravitreal injection of disperse increased leukocyte-endothelial interactions in the iridial microcirculation, a step which precedes the transendothelial migration of leukocytes into the affected tissue (Rom et al., 2013). Treatment of animals with the CB2R agonist, HU308, significantly decreased adhesion of leukocytes to the endothelium. These results are consistent with a study by Xu et al. (2007) who reported that CB2R agonists are anti-inflammatory in a model of EAU and reduce leukocyte trafficking (rolling and adhesion) to the inflamed retina. These authors further suggested that the anti-inflammatory effects of CB2R activation were mediated, in part, via decreased expression of cell surface adhesion molecules (lymphocyte function-associated antigen 1 (LFA-1) and P-selectin glycoprotein ligand 1 (PSGL-1), which mediate adhesion and rolling respectively (Xu et al., 2007).

In conclusion, our study demonstrated that the activation of CB2R attenuates the ocular pathology associated with the development and progression of experimental PVR. Activation of CB2R improved the overall morphology of the ocular tissues and decreased the number of activated retinal MG. We also showed that the levels of the pro-inflammatory cytokines in experimental PVR is elevated in the animals lacking CB2R compared to WT animals, suggesting that the presence and endogenous activation of CB2R may limit the ocular inflammatory response. Additionally, we demonstrated that ligands that activate CB2R attenuate leukocyte adhesion to iridial microvasculature in disperse-induced PVR, consistent with an anti-inflammatory role for this receptor. Our results suggest that drugs targeting CB2R may have utility in the treatment of PVR by diminishing the inflammatory response, and preventing consequent tissue damage.

Conflict of interest

MEM Kelly is a founding director of Panag Pharma Inc., a start-up company developing non-psychotropic cannabinoids for pain and inflammation.

Appendix A. Supplementary data

Supplementary data related to this article can be found at <http://dx.doi.org/10.1016/j.neuropharm.2016.08.030>.

References

- Aaberg, T.M., 1988. Management of anterior and posterior proliferative vitreoretinopathy. XLV. Edward Jackson memorial lecture. *Am. J. Ophthalmol.* 106, 519–532. [http://dx.doi.org/10.1016/0002-9394\(88\)90580-6](http://dx.doi.org/10.1016/0002-9394(88)90580-6).
- Agarwal, R.K., Silver, P.B., Caspi, R.R., 2012. Rodent models of experimental autoimmune uveitis. *Methods Mol. Biol.* 900, 1–28. http://dx.doi.org/10.1007/978-1-60761-720-4_22.
- Akhmetshina, A., Dees, C., Busch, N., Beer, J., Sarter, K., Zwerina, J., Zimmer, A., Distler, O., Schett, G., Distler, J.H.W., 2009. The cannabinoid receptor CB2 exerts antifibrotic effects in experimental dermal fibrosis. *Arthritis Rheum.* 60, 1129–1136. <http://dx.doi.org/10.1002/art.24395>.
- Ashton, J.C., Glass, M., 2007. The cannabinoid CB2 receptor as a target for inflammation-dependent neurodegeneration. *Curr. Neuropharmacol.* 5, 73–80.
- Bali, E., Feron, E.J., Peperkamp, E., Veckeneer, M., Mulder, P.G., van Meurs, J.C., 2010. The effect of a preoperative subconjunctival injection of dexamethasone on blood-retinal barrier breakdown following scleral buckling retinal detachment

- surgery: a prospective randomized placebo-controlled double blind clinical trial. *Graefes Arch. Clin. Exp. Ophthalmol.* 248, 957–962. <http://dx.doi.org/10.1007/s00417-010-1319-8>.
- Benito, C., Núñez, E., Tolón, R.M., Carrier, E.J., Rábano, A., Hillard, C.J., Romero, J., 2003. Cannabinoid CB2 receptors and fatty acid amide hydrolase are selectively overexpressed in neuritic plaque-associated glia in Alzheimer's disease brains. *J. Neurosci.* 23, 11136–11141.
- Boche, D., Perry, V.H., Nicoll, J.A.R., 2013. Review: activation patterns of microglia and their identification in the human brain. *Neuropathol. Appl. Neurobiol.* 39, 3–18. <http://dx.doi.org/10.1111/nan.12011>.
- Cantó Soler, M.V., Gallo, J.E., Dodds, R. A., Suburo, A.M., 2002. A mouse model of proliferative vitreoretinopathy induced by dispase. *Exp. Eye Res.* 75, 491–504. <http://dx.doi.org/10.1006/exer.2002.2031>.
- Carlisle, S.J., Marciano-Cabral, F., Staab, A., Ludwick, C., Cabral, G.A., 2002. Differential expression of the CB2 cannabinoid receptor by rodent macrophages and macrophage-like cells in relation to cell activation. *Int. Immunopharmacol.* 2, 69–82. [http://dx.doi.org/10.1016/S1567-5769\(01\)00147-3](http://dx.doi.org/10.1016/S1567-5769(01)00147-3).
- Carrier, E.J., Kearns, C.S., Barkmeier, A.J., Breese, N.M., Yang, W., Nithipatikom, K., Pfister, S.L., Campbell, W.B., Hillard, C.J., 2004. Cultured rat microglial cells synthesize the endocannabinoid 2-arachidonylglycerol, which increases proliferation via a CB2 receptor-dependent mechanism. *Mol. Pharmacol.* 65, 999–1007. <http://dx.doi.org/10.1124/mol.65.4.999>.
- Chen, W., Chen, H., Hou, P., Fok, A., Hu, Y., Lam, D.S.C., 2011. Midterm results of low-dose intravitreal triamcinolone as adjunctive treatment for proliferative vitreoretinopathy. *Retina* 31, 1137–1142. <http://dx.doi.org/10.1097/IAE.0b013e3181fe5427>.
- Diddie, K.R., Azen, S.P., Freeman, H.M., Boone, D.C., Aaberg, T.M., Lewis, H., Radtke, N.D., Ryan, S.J., 1996. Anterior proliferative vitreoretinopathy in the silicone study. Silicone study report number 10. *Ophthalmology* 103, 1092–1099. [http://dx.doi.org/10.1016/S0161-6420\(96\)30562-9](http://dx.doi.org/10.1016/S0161-6420(96)30562-9).
- Downer, E.J., 2011. Cannabinoids and innate immunity: taking a toll on neuroinflammation. *Sci. World J.* 11, 855–865. <http://dx.doi.org/10.1100/tsw.2011.84>.
- El-Ghrably, I.A., Dua, H.S., Orr, G.M., Fischer, D., Tighe, P.J., 2001. Intravitreal invading cells contribute to vitreal cytokine milieu in proliferative vitreoretinopathy. *Br. J. Ophthalmol.* 85, 461–470. <http://dx.doi.org/10.1136/bjo.85.4.461>.
- Eljaschewitsch, E., Witting, A., Mawrin, C., Lee, T., Schmidt, P.M., Wolf, S., Hoertnagl, H., Raine, C.S., Schneider-Stock, R., Nitsch, R., Ullrich, O., 2006. The endocannabinoid anandamide protects neurons during CNS inflammation by induction of MKP-1 in microglial cells. *Neuron* 49, 67–79. <http://dx.doi.org/10.1016/j.neuron.2005.11.027>.
- Fernández-Ruiz, J., Romero, J., Velasco, G., Tolón, R.M., Ramos, J.A., Guzmán, M., 2007. Cannabinoid CB2 receptor: a new target for controlling neural cell survival? *Trends Pharmacol. Sci.* 28, 39–45. <http://dx.doi.org/10.1016/j.tips.2006.11.001>.
- Fernández-Ruiz, J., Moro, M.A., Martínez-Orgado, J., 2015. Cannabinoids in neurodegenerative disorders and stroke/brain trauma: from preclinical models to clinical applications. *Neurotherapeutics* 12, 793–806. <http://dx.doi.org/10.1007/s13311-015-0381>.
- Galiegue, S., Mary, S., Marchand, J., Dussossoy, D., Carriere, D., Carayon, P., Bouaboula, M., Shire, D., Le Fur, G., Casellas, P., 1995. Expression of central and peripheral cannabinoid receptors in human immune tissues and leukocyte subpopulations. *Eur. J. Biochem.* 232, 54–61. <http://dx.doi.org/10.1111/j.1432-1033.1995.tb02780.x>.
- Gebremeskel, S., LeVatte, T., Liwski, R.S., Johnston, B., Bezuhly, M., 2015. The reversible P2Y12 inhibitor ticagrelor inhibits metastasis and improves survival in mouse models of cancer. *Int. J. Cancer* 136, 234–240. <http://dx.doi.org/10.1002/ijc.28947>.
- Gonsiorek, W., Lunn, C., Fan, X., Narula, S., Lundell, D., Hipkin, R.W., 2000. Endocannabinoid 2-arachidonyl glycerol is a full agonist through human type 2 cannabinoid receptor: antagonism by anandamide. *Mol. Pharmacol.* 57, 1045–1050. PMID: 10779390.
- Griffin, G., Wray, E.J., Tao, Q., McAllister, S.D., Rorrer, W.K., Aung, M., Martin, B.R., Abood, M.E., 1999. Evaluation of the cannabinoid CB2 receptor-selective antagonist, SR144528: further evidence for cannabinoid CB2 receptor absence in the rat central nervous system. *Eur. J. Pharmacol.* 377, 1117–1125. [http://dx.doi.org/10.1016/S0014-2999\(99\)00402-1](http://dx.doi.org/10.1016/S0014-2999(99)00402-1).
- Kersey, J.P., Broadway, D.C., 2006. Corticosteroid-induced glaucoma: a review of the literature. *Eye* 20, 407–416. <http://dx.doi.org/10.1038/sj.eye.6701895>.
- Khan, M.A., Brady, C.J., Kaiser, R.S., 2015. Clinical management of proliferative vitreoretinopathy: an update. *Retina* 35, 165–175. <http://dx.doi.org/10.1097/IAE.0000000000000447>.
- Kilkenny, C., Browne, W., Cuthill, I.C., Emerson, M., Altman, D.G., 2010. Animal research: reporting in vivo experiments: the ARRIVE guidelines. *Br. J. Pharmacol.* 160, 1577–1579. <http://dx.doi.org/10.1111/j.1476-5381.2010.00872.x>.
- Kon, C.H., Occleston, N.L., Aylward, G.W., Khaw, P.T., 1999. Expression of vitreous cytokines in proliferative vitreoretinopathy: a prospective study. *Investig. Ophthalmol. Vis. Sci.* 40, 705–712.
- Kreitzer, F.R., Stella, N., 2009. The therapeutic potential of novel cannabinoid receptors. *Pharmacol. Ther.* 122, 83–96. <http://dx.doi.org/10.1016/j.pharmthera.2009.01.005>.
- Lehmann, C., Kianian, M., Zhou, J., Cerny, V., Kelly, M., 2011. The endocannabinoid system in sepsis—a potential target to improve microcirculation? *Signa Vitae* 6, 7–13. Available from: <http://www.signavitae.com/2011/05/the-endocannabinoid-system-in-sepsis-a-potential-target-to-improve-microcirculation/>.
- Lehmann, C., Kianian, M., Zhou, J., Küster, I., Kuschneret, R., Whynt, S., Hung, O., Shukla, R., Johnston, B., Cerny, V., Pavlovic, D., Spassov, A., Kelly, M.E., 2012. Cannabinoid receptor 2 activation reduces intestinal leukocyte recruitment and systemic inflammatory mediator release in acute experimental sepsis. *Crit. Care* 16, 1–22. <http://dx.doi.org/10.1186/cc11248>.
- Lei, H., Hovland, P., Velez, G., Haran, A., Gilbertson, D., Hirose, T., Kazlauskas, A., 2007. A potential role for PDGF-C in experimental and clinical proliferative vitreoretinopathy. *Investig. Ophthalmol. Vis. Sci.* 48, 2335–2342. <http://dx.doi.org/10.1167/jovs.06-0965>.
- Lopez-Rodriguez, A.B., Siopi, E., Finn, D.P., Marchand-Leroux, C., Garcia-Segura, L.M., Jafarian-Tehrani, M., Viveros, M.-P., 2015. CB1 and CB2 cannabinoid receptor antagonists prevent minocycline-induced neuroprotection following traumatic brain injury in mice. *Cereb. Cortex* 25, 35–45. <http://dx.doi.org/10.1093/cercor/bht202>.
- Lu, Q., Straiker, A., Lu, Q., Maguire, G., 2000. Expression of CB2 cannabinoid receptor mRNA in adult rat retina. *Vis. Neurosci.* 17, 91–95. PMID: 10750830.
- Machemer, R., Aaberg, T., Freeman, M., Irvine, A.R., Lean, J., Michels, R.M., 1991. An update classification of retinal detachment with proliferative vitreoretinopathy. *Am. J. Ophthalmol.* 112, 159–165. PMID: 1867299.
- Mandava, N., Blackburn, P., Paul, D.B., Wilson, M.W., Read, S.B., Alspaugh, E., Tritz, R., Barber, J.R., Robbins, J.M., Kruse, C.A., 2002. Ribozyme to proliferative cell nuclear antigen to treat proliferative vitreoretinopathy. *Investig. Ophthalmol. Vis. Sci.* 43, 3338–3348. PMID: 12356843.
- Maneu, V., Noailles, A., Gómez-Vicente, V., Carpena, N., Cuenca, N., Gil, M.L., Gozalbo, D., 2016. Immunosuppression, peripheral inflammation and invasive infection from endogenous gut microbiota activate retinal microglia in mouse models. *Microbiol. Immunol.* <http://dx.doi.org/10.1111/1348-0421.12405>.
- Maneu, V., Noailles, A., Megias, J., Gómez-Vicente, V., Carpena, N., Cuenca, N., Gil, M.L., Gozalbo, D., Cuenca, N., 2014. Retinal microglia are activated by systemic fungal infection. *Investig. Ophthalmol. Vis. Sci.* 55, 3578–3585. <http://dx.doi.org/10.1167/jovs.14-14051>.
- Maresz, K., Carrier, E.J., Ponomarev, E.D., Hillard, C.J., Dittel, B.N., 2005. Modulation of the cannabinoid CB2 receptor in microglial cells in response to inflammatory stimuli. *J. Neurochem.* 95, 437–445. <http://dx.doi.org/10.1111/j.1471-4159.2005.03380.x>.
- Martínez-Orgado, J., Fernández-López, D., Lizaola, I., Romero, J., 2007. The seek of neuroprotection: introducing cannabinoids. *Recent Pat. CNS Drug Discov.* 2, 131–139. <http://dx.doi.org/10.2174/157488907780832724>.
- McGrath, J.C., Drummond, G.B., McLachlan, E.M., Kilkenny, C., Wainwright, C.L., 2010. Editorial: guidelines for reporting experiments involving animals: the ARRIVE guidelines. *Br. J. Pharmacol.* 160, 1573–1576. <http://dx.doi.org/10.1111/j.1476-5381.2010.00873.x>.
- McPartland, J.M., Duncan, M., Di Marzo, V., Pertwee, R., 2015. Are cannabidiol and (Δ⁹)-tetrahydrocannabinol negative modulators of the endocannabinoid system? A systematic review. *Br. J. Pharmacol.* 172, 737–753. <http://dx.doi.org/10.1111/bph.12944>.
- Mechoulam, R., Panikashvili, D., Shohami, E., 2002. Cannabinoids and brain injury: therapeutic implications. *Trends Mol. Med.* 8, 58–61. [http://dx.doi.org/10.1016/S1471-4914\(02\)00276-1](http://dx.doi.org/10.1016/S1471-4914(02)00276-1).
- Mechoulam, R., Parker, L.A., 2013. The endocannabinoid system and the brain. *Annu. Rev. Psychol.* 64, 21–47. <http://dx.doi.org/10.1146/annurev-psych-113011-143739>.
- Morales, P., Hernandez-Folgado, L., Goya, P., Jagerovic, N., 2016. Cannabinoid receptor 2(CB2) agonists and antagonists: a patent update. *Expert Opin. Ther. Pat.* 26, 843–856. <http://dx.doi.org/10.1080/13543776.2016.1193157>.
- Morescalchi, F., Duse, S., Gambicorti, E., Romano, M.R., Costagliola, C., Semeraro, F., 2013. Proliferative vitreoretinopathy after eye injuries: an overexpression of growth factors and cytokines leading to a retinal keloid. *Mediat. Inflamm.* 2013, 1–12. <http://dx.doi.org/10.1155/2013/269787>.
- Morrison, H.W., Filosa, J.A., 2013. A quantitative spatiotemporal analysis of microglia morphology during ischemic stroke and reperfusion. *J. Neuroinflammation* 10, 4. <http://dx.doi.org/10.1186/1742-2094-10-4>.
- Munoz-Luque, J., Ros, J., Fernandez-Varo, G., Tugues, S., Morales-Ruiz, M., Alvarez, C.E., Friedman, S.L., Arroyo, V., Jimenez, W., 2007. Regression of fibrosis after chronic stimulation of cannabinoid CB2 receptor in cirrhotic rats. *J. Pharmacol. Exp. Ther.* 324, 475–483. <http://dx.doi.org/10.1124/jpet.107.131896>.
- Munro, S., Thomas, K.L., Abu-Shaar, M., 1993. Molecular characterization of peripheral receptor for cannabinoids. *Nature* 365, 61–65. <http://dx.doi.org/10.1038/365061a0>.
- Palazuelos, J., Aguado, T., Pazos, M.R., Julien, B., Carrasco, C., Resel, E., Sagredo, O., Benito, C., Romero, J., Azcoitia, I., Fernandez-Ruiz, J., Guzmán, M., Galve-Roperh, I., 2009. Microglial CB2 cannabinoid receptors are neuroprotective in Huntington's disease excitotoxicity. *Brain* 132, 3152–3164. <http://dx.doi.org/10.1093/brain/awp239>.
- Palazuelos, J., Davoust, N., Julien, B., Hatterer, E., Aguado, T., Mechoulam, R., Benito, C., Romero, J., Silva, A., Guzmán, M., Nataf, S., Galve-Roperh, I., 2008. The CB2 Cannabinoid Receptor Controls Myeloid Progenitor Trafficking: involvement in the pathogenesis of an animal model of multiple sclerosis. *J. Biol. Chem.* 283, 13320–13329. <http://dx.doi.org/10.1074/jbc.M707960200>.
- Pastor, J.C., 1998. Proliferative vitreoretinopathy: an overview. *Surv. Ophthalmol.* 43, 3–18. [http://dx.doi.org/10.1016/S0039-6257\(98\)00023-X](http://dx.doi.org/10.1016/S0039-6257(98)00023-X).
- Pastor, J.C., de la Rúa, E.R., Martín, F., 2002. Proliferative vitreoretinopathy: risk factors and pathobiology. *Prog. Retin. Eye Res.* 21, 127–144. [http://dx.doi.org/10.1016/S1350-9462\(01\)00023-4](http://dx.doi.org/10.1016/S1350-9462(01)00023-4).
- Patel, N.N., Bunce, C., Asaria, R.H., Charteris, D.G., 2004. Resources involved in

- managing retinal detachment complicated by proliferative vitreoretinopathy. *Retina* 24, 883–887. PMID: 15579985.
- Pryce, G., Baker, D., 2015. Endocannabinoids in multiple sclerosis and amyotrophic lateral sclerosis. *Handb. Exp. Pharmacol.* 231, 213–231. http://dx.doi.org/10.1007/978-3-319-20825-1_7.
- Rajesh, M., Mukhopadhyay, P., Bátkai, S., Haskó, G., Liaudet, L., Huffman, J.W., Csiszar, A., Ungvari, Z., Mackie, K., Chatterjee, S., Pacher, P., 2007. CB2-receptor stimulation attenuates TNF-alpha-induced human endothelial cell activation, transendothelial migration of monocytes, and monocyte-endothelial adhesion. *Am. J. Physiol. Heart Circ. Physiol.* 293, 2210–2218. <http://dx.doi.org/10.1152/ajpheart.00688.2007>.
- Rajesh, M., Mukhopadhyay, P., Bátkai, S., Patel, V., Saito, K., Matsumoto, S., Kashiwaya, Y., Horváth, B., Mukhopadhyay, B., Becker, L., Haskó, G., Liaudet, L., Wink, D.A., Veves, A., Mechoulam, R., Pacher, P., 2010. Cannabidiol attenuates cardiac dysfunction, oxidative stress, fibrosis, and inflammatory and cell death signaling pathways in diabetic cardiomyopathy. *J. Am. Coll. Cardiol.* 56, 2115–2125. <http://dx.doi.org/10.1016/j.jacc.2010.07.033>.
- Ramirez, B.G., Blázquez, C., Gómez del Pulgar, T., Guzmán, M., de Ceballos, M.L., 2005. Prevention of Alzheimer's disease pathology by cannabinoids: neuroprotection mediated by blockade of microglial activation. *J. Neurosci.* 25, 1904–1913. <http://dx.doi.org/10.1523/JNEUROSCI.4540-04.2005>.
- Rom, S., Persidsky, Y., 2013. Cannabinoid receptor 2: potential role in immunomodulation and neuroinflammation. *J. Neuroimmune Pharmacol.* 8, 608–620. <http://dx.doi.org/10.1007/s11481-013-9445-9>.
- Rom, S., Zuluaga-Ramirez, V., Dykstra, H., Reichenbach, N.L., Pacher, P., Persidsky, Y., 2013. Selective activation of cannabinoid receptor 2 in leukocytes suppresses their engagement of the brain endothelium and protects the blood-brain barrier. *Am. J. Pathol.* 183, 1548–1558. [http://dx.doi.org/10.1016/S1471-4914\(12\)02276-1](http://dx.doi.org/10.1016/S1471-4914(12)02276-1).
- Sadaka, A., Giuliani, G.P., 2012. Proliferative vitreoretinopathy: current and emerging treatments. *Clin. Ophthalmol.* 6, 1325–1333. <http://dx.doi.org/10.2147/OPHT.S27896>.
- Sagredo, O., González, S., Aroyo, I., Pazos, M.R., Benito, C., Lastres-Becker, I., Romero, J.P., Tolón, R.M., Mechoulam, R., Brouillet, E., Romero, J., Fernández-Ruiz, J., 2009. Cannabinoid CB2 receptor agonists protect the striatum against malonate toxicity: relevance for Huntington's disease. *Glia* 57, 1154–1167. <http://dx.doi.org/10.1002/glia.20838>.
- Schatz, A.R., Lee, M., Condie, R.B., Pulaski, J.T., Kaminski, N.E., 1997. Cannabinoid receptors CB1 and CB2: a characterization of expression and adenylyl cyclase modulation. *Toxicol. Appl. Pharmacol.* 142, 278–287. <http://dx.doi.org/10.1006/taap.1996.8034>.
- Schley, M., Stander, S., Kerner, J., Vajkoczy, P., Schupfer, G., Dusch, M., Schmelz, M., Konrad, C., 2009. Predominant CB2 receptor expression in endothelial cells of glioblastoma in humans. *Brain Res. Bull.* 79, 333–337. <http://dx.doi.org/10.1016/j.brainresbull.2009.01.011>.
- Shmest, Y.A., Goncharov, I., Eichler, M., Shneyvays, V., Isaac, A., Vogel, Z., Shainberg, A., 2006. Delta-9-tetrahydrocannabinol protects cardiac cells from hypoxia via CB2 receptor activation and nitric oxide production. *Mol. Cell. Biochem.* 283, 75–83. <http://dx.doi.org/10.1007/s11010-006-2346-y>.
- Stella, N., 2011. Cannabinoid and cannabinoid-like receptors in microglia, astrocytes and astrocytomas. *Glia* 58, 1017–1030. <http://dx.doi.org/10.1002/glia.20983>.
- Stence, N., Waite, M., Dailey, M.E., 2001. Dynamics of microglial activation: a confocal time-lapse analysis in hippocampal slices. *Glia* 33, 256–266. doi: 10.1002/1098-1136(200103)33:3<256::AID-GLIA1024>3.0.CO;2-J.
- Storr, M.A., Keenan, C.M., Zhang, H., Patel, K.D., Makriyannis, A., Sharkey, K.A., 2009. Activation of the cannabinoid 2 receptor (CB2) protects against experimental colitis. *Inflamm. Bowel Dis.* 15, 1678–1685. <http://dx.doi.org/10.1002/ibd.20960>.
- Streit, W.J., Walter, S.A., Pennell, N.A., 1999. Reactive microgliosis. *Prog. Neurobiol.* 57, 563–581. [http://dx.doi.org/10.1016/S0301-0082\(98\)00069-0](http://dx.doi.org/10.1016/S0301-0082(98)00069-0).
- Takaki, J., Fujimori, K., Miura, M., Suzuki, T., Sekino, Y., Sato, K., 2012. L-glutamate released from activated microglia downregulates astrocytic L-glutamate transporter expression in neuroinflammation: the “collusion” hypothesis for increased extracellular L-glutamate concentration in neuroinflammation. *J. Neuroinflammation* 9, 275. <http://dx.doi.org/10.1186/1742-2094-9-275>.
- Tan, J., Liu, Y., Li, W., Gao, Q., 2012. Ocular pathogenesis and immune reaction after intravitreal dispase injection in mice. *Mol. Vis.* 18, 887–900. PMID: 22511850.
- Tanasescu, R., Constantinescu, C.S., 2010. Cannabinoids and the immune system: an overview. *Immunobiology* 215, 588–597. <http://dx.doi.org/10.1016/j.imbio.2009.12.005>.
- Toguri, J.T., Lehmann, C., Laprairie, R.B., Szczesniak, A. M., Zhou, J., Donovan-Wright, E.M., Kelly, M.E.M., 2014. Anti-inflammatory effects of cannabinoid CB2 receptor activation in endotoxin-induced uveitis. *Br. J. Pharmacol.* 171, 1448–1461. <http://dx.doi.org/10.1111/bph.12545>.
- Turgut, B., Guler, M., Akpolat, N., Demir, T., Celiker, U., 2011. The impact of tacrolimus on vascular endothelial growth factor in experimental corneal neovascularization. *Curr. Eye Res.* 36, 34–40. <http://dx.doi.org/10.3109/02713683.2010.516620>.
- Walter, L., Franklin, A., Witting, A., Wade, C., Xie, Y., Kunos, G., Mackie, K., Stella, N., 2003. Nonpsychotropic cannabinoid receptors regulate microglial cell migration. *J. Neurosci.* 23, 1398–1405. PMID: 12598628.
- Xu, H., Cheng, C.L., Chen, M., Manivannan, A., Cabay, L., Pertwee, R.G., Coutts, A., Forrester, J.V., 2007. Anti-inflammatory property of the cannabinoid receptor-2-selective agonist JWH-133 in a rodent model of autoimmune uveoretinitis. *J. Leukoc. Biol.* 82, 532–541. <http://dx.doi.org/10.1189/jlb.0307159>.
- Zhang, J., Hoffert, C., Vu, H.K., Groblewski, T., Ahmad, S., O'Donnell, D., 2003. Induction of CB2 receptor expression in the rat spinal cord of neuropathic but not inflammatory chronic pain models. *Eur. J. Neurosci.* 17, 2750–2754. <http://dx.doi.org/10.1046/j.1460-9568.2003.02704.x>.
- Zhang, W., Tan, J., Liu, Y., Li, W., Gao, Q., Lehmann, P.V., 2012. Assessment of the innate and adaptive immune system in proliferative vitreoretinopathy. *Eye* 26, 872–881. <http://dx.doi.org/10.1038/eye.2012.52>.